PROFESSOR PAUL WILLIAM JAMES TAYLOR (Orcid ID : 0000-0003-3076-2084)

Received Date : 19-Feb-2017

Revised Date : 07-Apr-2017

Accepted Date : 18-Apr-2017

Article type : Original Article

Running head recto: Two new species of Paraphoma

Running head verso: A. Moslemi et al.

Paraphoma chlamydocopiosa sp. nov. and *Paraphoma pye* sp. nov., two new species associated with leaf and crown infection of pyrethrum

A. Moslemi[a], P. K. Ades[b], P. W. Crous[ac], T. Groom[d], J. B. Scott[e], M. E. Nicolas[a] and P. W. J. Taylor[a]*

[a]*Faculty of Veterinary and Agricultural Sciences, University of Melbourne, Victoria, 3010;* [b]*School of Ecosystem and Forest Sciences, University of Melbourne, Victoria, 3010, Australia;* [c]*Westerdijk Fungal Biodiversity Institute, Utrecht, Netherlands;* [d]*Botanical Resources Australia Pty Ltd, Ulverstone, Tasmania, 7315; and* [e]*Tasmanian Institute of Agriculture, University of Tasmania – Cradle Coast Campus, Burnie, Tasmania, 7320, Australia*

*****E-mail: paulwjt@unimelb.edu.au

Two new pathogens of pyrethrum, described as *Paraphoma chlamydocopiosa* and *Paraphoma pye*, isolated from necrotic leaf lesions on pyrethrum plants in northern Tasmania, Australia, were identified using morphological characters, phylogenetic analysis of

the internal transcribed spacer (ITS), elongation factor 1-α (*EF1*-α) and β-tubulin (*TUB)* genes, and pathogenicity bioassays. Bootstrap support in the combined and individual gene region phylogenetic trees supported the two species that were significantly different from the closely related *P. chrysanthemicola* and *P. vinacea*. Morphological characteristics also supported the two new species, with conidia of *P. chlamydocopiosa* being considerably longer and wider than either *P. chrysanthemicola* or *P. vinacea*, and *P. pye* being distinct in forming bilocular pycnidia. Glasshouse pathogenicity tests based on root dip inoculation resulted in *P. chlamydocopiosa* and *P. pye* infecting the crown and upper root tissues of pyrethrum plants, and significant reduction in biomass 2 months after inoculation. Both of these *Paraphoma* species caused leaf lesions during *in vitro* and *in vivo* bioassays 2 weeks after foliar spray inoculation. Although *P. chlamydocopiosa* and *P. pye* were shown to be crown rot pathogens, they were also commonly isolated from leaves of diseased plants in pyrethrum fields of northern Tasmania.

Keywords: bilocular pycnidia, longer conidia, *Paraphoma chlamydocopiosa*, *Paraphoma pye*, pathogenicity, phylogenetic analysis

Introduction

Pyrethrum (*Tanacetum cinerariifolium*) is a perennial in the Asteraceae that has been widely used for pyrethrin production. Insecticidal pyrethrins are extracted from the achenes within the flower heads (Grdisa *et al.*, 2009). The majority of the world's production of natural pyrethrins occurs in Victoria and northern Tasmania. The crop is spring sown, with its first harvest occurring approximately 15 months after establishment and up to three subsequent annual harvests thereafter (Vaghefi *et al.*, 2016).

Many foliar and soilborne diseases of pyrethrum affect flower production and regrowth potential. The most important foliar diseases of pyrethrum are ray blight caused by *Stagonosporopsis tanaceti* (Vaghefi *et al.*, 2016; Bhuiyan *et al.*, 2017), tan spot that is predominantly caused by *Didymella tanaceti* (Pearce *et al.*, 2015), anthracnose caused by *Colletotrichum tanaceti* (Barimani *et al.*, 2013) and sclerotinia flower blight caused by *Sclerotinia minor* (O'Malley *et al*., 2015). Soilborne pathogens of pyrethrum include sclerotinia crown rot caused by *S. sclerotiorum* (Pethybridge *et al*., 2008), *Paraphoma vinacea* that causes crown rot and reduced growth in yield decline-affected fields of northern

Tasmania (Moslemi *et al.*, 2016), and *Fusarium oxysporum* and *F. avenaceum* associated with yield decline of pyrethrum (Moslemi *et al.*, 2017).

The taxon *Paraphoma* was originally introduced as a section of the genus *Phoma*, but was later raised to a genus distinguished by production of setose pycnidia and dictyochlamydospores (Aveskamp *et al.*, 2010; De Gruyter *et al.*, 2013). However, based on phylogenetic studies several species were also allocated to genera in closely related families such as Coniothyriaceae, Cucurbitariaceae and Phaeosphaeriaceae (Chen *et al.*, 2015).

Paraphoma species have been identified mainly as soilborne pathogens, causing root and crown rot diseases in temperate areas of Australia, America and Eurasia (Boerema *et al.*, 2004; De Gruyter *et al.*, 2013; Moslemi *et al.*, 2016). The type species, *P. radicina*, was first identified on roots of *Prunus cerasus* in 1901 in Australia (De Gruyter *et al.*, 2010). *Paraphoma radicina* was also isolated from *Malus sylvestris* in the Netherlands and *Lycopersicon esculentum* (now *Solanum lycopersicum*) in Germany in 1907 (De Gruyter *et al.*, 2010). The type isolate of *Paraphoma fimeti* was isolated from soil and recovered from the roots of *Juniperus communis* in 1991 in Switzerland (De Gruyter *et al.*, 2010). *Paraphoma chrysanthemicola* was the first member of *Paraphoma* reported on plants of other *Compositae* (De Gruyter *et al.*, 2010). Srivastava (1953) also reported this species as a pathogen of *Chrysanthemum* sp. Roots of *Chrysanthemum morifolium* were found to be infected with *P. chrysanthemicola* in 1967 in Germany (De Gruyter *et al.*, 2010). Later, Dorenbosch (1970) reported *P. chrysanthemicola* as a root pathogen of florists' *Chrysanthemum*. Other *Paraphoma* species have also been reported to be pathogens of Compositae such as *C. morifolium* and *Cichorium intybus*, and *Calluna vulgaris* (Ericaceae) (Ge *et al.*, 2016). Hay *et al.* (2015) reported *P. chrysanthemicola* as a pathogen causing necrotic leaf spots at low frequency in pyrethrum fields of northern Tasmania. However, the existence and pathogenicity of *P. chrysanthemicola* to pyrethrum in Australia was not verified.

This research describes two new *Paraphoma* species isolated from pyrethrum leaf lesions in northern Tasmania, Australia using taxonomic and multigene phylogenetic studies and assesses pathogenicity of these species in pyrethrum as foliar and crown pathogens.

Materials and methods

Isolates

Sixteen *Paraphoma* isolates were selected from different geographical locations in northern Tasmania. This included four *Paraphoma* isolates (BRIP 65168, BRIP 65169, BRIP 65170 and BRIP 65171) isolated from leaf lesions by N. Vaghefi in 2013 from pyrethrum plants at Table Cape and eight isolates collected by T. Pearce, F. Hay and J. Scott between 2012 and 2014 from pyrethrum leaf lesions (BRIP 57988, BRIP 57989, BRIP 65173, BRIP 65174, BRIP 65176, BRIP 65177, BRIP 65178 and BRIP 65179), which were identified at that time to be *P. chrysanthemicola* by Hay *et al.* (2015). Four *P. vinacea* isolates (BRIP 63684, BRIP 63683, BRIP 63682 and BRIP 63685) collected by A. Moslemi in 2014 from infected crown tissues of yield-decline affected pyrethrum plants at Devonport were also included. Details of the sites and collectors have been provided in Table 1. Sequences of five *P. fimeti* isolates, CBS 164.31, CBS 119754, CBS 258.68, CBS 550.70 and CBS 379.67, received from Westerdijk Fungal Biodiversity Institute (CBS), Utrecht, Netherlands were also included. Other reference sequences used in the phylogenetic analyses were downloaded from GenBank at http://www.ncbi.nlm.nih.gov/ (Table 2).

Morphological analysis

One representative isolate from each of the phylogenetic clades of the Tasmanian *Paraphoma* were examined for their morphological characteristics. Isolates were examined for growth rate on oatmeal agar (OA), malt extract agar (MEA), cherry decoction agar (CHA), potato dextrose agar (PDA) and V8 juice agar (V8) (Crous *et al.*, 2009), after 7 days' incubation according to the conditions described by Boerema *et al.* (2004). Three replicates per isolate were used. Colony colour was assessed on all media after 2 weeks using Rayner's colour chart (Rayner, 1970).

Additionally, all isolates grown on CHA, OA and MEA for 14 days at 20–22 °C and under the light regime according to Boerema *et al.* (2004) were examined for the production of pycnidia and conidia. Two isolates (BRIP 65168 and 65170), which did not produce pycnidia on these media, were also grown on PDA and V8 to induce pycnidial production. Pycnidia were examined for the presence/absence of setae and/or ostioles. The pycnidial cell wall anatomy was observed by sectioning individual pycnidia using a RM2125 RTS microtome (Leica) as described by Moslemi *et al.* (2016). Conidial shape and dimensions

(length × width) were also recorded. In each measurement, 30 replicates of each fungal structure were measured from samples mounted in clear lactic acid (Aveskamp *et al.*, 2010) using a DM-2900 (Leica) compound microscope. Microscopic images were captured with differential interference contrast and bright-field illumination.

In addition, to determine the E metabolite production and cell wall anatomy of isolates, 1 M NaOH and iodine reaction tests were carried out, respectively, according to Boerema *et al.* (2004) and *Phoma* methodologies (http://www.q-bank.eu).

PCR and sequencing

Total genomic DNA was extracted from mycelium scraped directly from 7-day-old, single-spored cultures grown on OA using the DNeasy Plant Mini kit (QIAGEN) following the manufacturer's instructions. All PCR amplifications for ITS, *TUB* and *EF1* were performed in a MyCycler thermal cycler (Bio-Rad) with a total reaction volume of 12.5 µL according to Moslemi *et al.* (2016). The PCR cycling conditions and product purifications were performed as described in Moslemi *et al.* (2016). Agarose gels were stained with a SYBR Safe DNA gel stain and visualized with a GelDoc (Bio-Rad) after electrophoresis.

Purified amplicons from each gene region were sequenced at the Australian Genome Research Facility Ltd, Melbourne, Australia. Amplicons were sequenced in both the forward and reverse sense using the same set of primers on a 3730xl DNA Analyzer (Applied Biosystems) and with BigDye Terminator v. 3.1 chemistry. Sequences of related genera for ITS, *TUB* and *EF1* were downloaded from the GenBank nucleotide database (Table 2). Consensus sequences were obtained from both forward and reverse sequences using the DENOVO assembly option and pairwise aligned with the CLUSTALW algorithm within GENEIOUS v. 7.1.9 (Biomatters Ltd.) (Kearse *et al.*, 2012) and annotated with the most similar gene sequences of *Paraphoma* species obtained from NCBI database within GENEIOUS. Sequences were submitted to GenBank and descriptions of nomenclature to MycoBank (Crous *et al.*, 2004).

Phylogenetic analysis

Maximum likelihood (ML) and neighbour-joining (NJ) phylogenetic trees were constructed for each gene individually and combined using GENEIOUS TREE BUILDER for NJ analysis within GENEIOUS and PHYML for ML analysis (Guindon & Gascuel, 2003). A general time-reversible with invariant sites and gamma distributed rates across sites (GTR+I+G) was determined as the best nucleotide substitution model for ML analysis in PAUP v. 4.0a151 (Swofford, 2003) based on the Akaike information criterion (AIC) and Bayesian information criterion (BIC) with 500 bootstrap replicates as default. Gaps were treated as missing data. For the NJ analysis, the Tamura–Nei substitution model (Tamura *et al.*, 2013) was selected as the best fit model with gamma distributed (G) rate among sites and pairwise deletion of the gaps using MEGA 6 (Tamura *et al.*, 2013) with 1000 bootstrap replicates to assess the relative stability of branches and comparing the AIC and BIC estimates. Congruence of the trees for each pair of genes was confirmed online at http://max2.ese.u-psud.fr/icong/index.help.html before concatenation and generating the combined phylogenetic tree (de Vienne *et al.*, 2007). GenBank accession numbers for reference markers *EF1*, *TUB* and ITS were derived from Quaedvlieg *et al.* (2013). Sequence alignments of *P. chlamydocopiosa* and *P. pye* (12 isolates) and combined phylogenetic trees were deposited in TreeBASE at www.treebase.org as submission 20959.

Pathogenicity tests

Pathogenicity of *Paraphoma* species isolated from pyrethrum plants was assessed in two experiments using root dip and foliar spray inoculation methods. For each experiment, seedlings of cultivar Pyrate were germinated from steam-sterilized seeds and raised in seedling mix in Tasmania at Botanical Resources Australia (BRA). Seedlings were transferred to 10 cm diameter pots with potting mix (Debco), fertilized with 5 g Osmocote Plus (Scotts Australia Pty Ltd) per pot and grown in a glasshouse for 2 months at 25–27 °C under natural light.

Inoculum was prepared from newly grown, single-spored cultures on PDA, by adding 10 mL sterile water to each plate and gently scraping the colony surface with a glass spreader and then filtering the spore suspension through cheesecloth. The concentration of each spore suspension was quantified to 10^6 spores mL^{-1} using a haemocytometer (Moslemi *et al.*, 2016). Two drops of 0.1% Tween 20 solution was added to each spore suspension to increase the ability of the spores to adhere to the surface of the inoculated tissue.

Root inoculation

Isolates BRIP 65168 and BRIP 65169 were chosen as representatives of all other isolates of the respective phylogenetic groups in this experiment based on the morphological similarities with other species in each clade. Holotype isolate *P. vinacea* BRIP 63684 was also included in the experiment for comparison. The pathogenicity experiment was conducted in duplicate.

In both experiments, 10 pyrethrum plants per treatment were root dip inoculated with the spore suspension for each isolate. Pyrethrum plants were uprooted and roots washed under tap water for 10 min to remove excess soil. Roots were then immersed in 100 mL of the spore suspension for 10 min. Thereafter, they were transplanted into 10 cm diameter pots and maintained in a glasshouse for 2 months. Controls were inoculated with sterile water but otherwise treated identically. To prevent cross contamination between treatments by airborne dispersal of spores, all experiments were carried out in a nonrandomized design with no random placement of the plants within treatments. True replication was achieved by repeating the experiments. The distance between different treatments was at least 70 cm and drip irrigation was used to minimize splash dispersal of spores.

Two months after inoculation, individual plants (n =10 per treatment) were removed from each pot and roots were washed under tap water to remove the excess soil. They were then transferred to the laboratory for sectioning. Tissue sectioning and surface sterilization were carried out as described by Moslemi *et al.* (2016). Sterilized tissues were subsequently cultured onto water agar (WA). After 4 days' incubation at 22–24 °C, colonies growing on WA were subcultured onto OA for identification (Crous *et al.*, 2009). Oatmeal agar plates were incubated at 22–24 °C in the dark for 7 days and then under a 13 h photoperiod with UV and white fluorescent light for 7 days (Boerema *et al.*, 2004).

After sampling and reisolation of the pathogen, the remaining plants (n = 10 per treatment) were sectioned into petioles and leaves (above ground), and crown and root (below ground). Plant samples were dried in an oven for 3 days at 71 °C and then weighed.

Leaf and petiole inoculation

Three replicates per treatment of healthy rosette stage Pyrate plants were spray inoculated with 20 mL (each plant) of 10^6 spores mL^{-1} spore suspension of each isolate (BRIP 65168, BRIP 65169 and BRIP 63684); control plants were sprayed with water. A hand sprayer was used to spray the leaves with inoculum until just before runoff. Each plant was then covered

with a plastic bag for 24 h to increase humidity after inoculation, to encourage spore germination and infection. Covers were then removed and plants were maintained in the glasshouse for 14 days until leaf lesions developed on the leaves. Any leaf with the lesions developed on both sides was detached and cultured for fungal identification during this period. Tissue surface sterilization and culturing were carried out as previously described. A DM205 FA stereomicroscope (Leica) was used to assess the disease symptoms.

In addition, an *in vitro* inoculation test with surface-sterilized detached petioles of healthy pyrethrum plants was carried out using the same isolates, by pipetting 10 µL of a 10^6 spores mL^{-1} suspension of each isolate onto the leaves and petioles. Controls were treated with sterile water. Detached petioles were incubated in plastic containers, four petioles per container, with moistened filter papers at 21 °C for 8 days. Symptoms were assessed after 8 days by observing the petioles under a dissecting microscope and tissue infection was confirmed by culturing the surface sterilized leaf tissues on WA and then subculturing onto OA. Both *in vivo* and *in vitro* tests were repeated.

Dry weight data analyses

Dry weight data (above ground, below ground and total) analyses were performed using a mixed model with the MIXED procedure in SAS v. 9.4 (SAS Institute Inc.) and applying the residual maximum likelihood (REML) estimation method. This permitted data from both experiments to be combined in one analysis. Noninfected plants, as determined by isolations, were removed from the data. Comparison of means was performed by pairwise *t*-tests (α = 0.05). SAS was used for all analyses. The linear mixed model fitted was:

$$Y_{ijk} = \mu + \tau_i + \gamma_j + \tau\gamma_{ij} + \varepsilon_{ijk}$$

where μ is the overall mean, τ_i is the fixed effect of treatment i, γ_j is the random effect of trial j, $\tau\gamma_{ij}$ is the random interaction between treatment i and trial j and ε_{ijk} is an independent random error. The variable ε is assumed to be normally distributed, with fixed variance within a trial, but may vary between trials. The interaction between treatment and trial ($\tau\gamma_{ij}$) was not significant by likelihood ratio test and hence was deleted from the final model. Data for plants that were inoculated but not confirmed to be infected were omitted from the analysis. This resulted in an unbalanced design.

Results

Phylogeny

Nucleotide sequences of 31 isolates were used in the three gene phylogenetic analyses. The congruence test between each pair of loci showed all to be congruent and hence all three genes could be included in the combined phylogenetic analysis ($P < 0.001$). Moreover, a congruence test between the NJ and ML phylogenetic trees showed tree topologies were identical and trees were more congruent than expected under random chance ($P < 0.001$).

In individual PHYML trees of ITS and *TUB*, BRIP 65169 and BRIP 65171 clustered with *P. vinacea* with 88% and 80% bootstrap support, respectively. However, in the tree constructed for *EF1* the two isolates clustered with *P. chrysanthemicola* with 88% bootstrap support. All other isolates (BRIP 65168 to BRIP 65179, BRIP 57988 and BRIP 57989) clustered in a separate monophyletic group with bootstrap values of 94%, 84% and 73% for ITS, *EF1* and *TUB*, respectively (individual trees are not shown). In the combined PHYML phylogenetic tree of ITS-*TUB*-*EF1*, a total of 828 (ITS: 373, *EF1*: 263, TUB: 192) characters in the final dataset were obtained including 618 (ITS: 297, *EF1*: 179, *TUB*: 142) constant characters, 155 (ITS: 57, *EF1*: 54, *TUB*: 44) parsimony informative characters and 55 uninformative variable characters. The three-gene phylogeny consisting of ITS, *TUB* and *EF1* showed two new species of *Paraphoma* in well-supported monophyletic clades, distinct from the previously described *Paraphoma* species. In the combined PHYML maximum likelihood phylogenetic tree, BRIP 65168 and BRIP 65170, which were recovered from leaf lesions in 2013 in Table Cape, clustered with the eight *Paraphoma* isolates including BRIP 65172 to BRIP 65179 and BRIP 57988 and BRIP 57989, collected from the leaf lesions between 2012 and 2014 in different geographical locations of northern Tasmania (Table 1), with 99% bootstrap support in PHYML and 100% support in NJ trees phylogenetic analyses. Two isolates, BRIP 65169 and BRIP 65171, fell in the same group as *P. chrysanthemicola* and *P. vinacea*, but formed a clade distinct from both these species in both the PHYML and NJ trees (Fig. 1). Neighbour-joining bootstrap values are shown where they differ from the PHYML values. Isolates BRIP 57988 and BRIP 57989 were previously used to identify *P. chrysanthemicola* by Hey *et al*. (2015) (BRIP accession numbers were assigned subsequent to the publication by Hey *et al*., 2015).

Morphology and taxonomy

Morphological traits differentiated the *Paraphoma* isolates into two distinct groups. Assignment of individuals to these groups matched perfectly the groups from the phylogenetic analyses, confirming that the *Paraphoma* isolated from leaf lesions of pyrethrum plants in the fields of northern Tasmania were two new species. The names *Paraphoma chlamydocopiosa* and *Paraphoma pye* are proposed for these. All isolates were compared with the type specimen of *P. chrysanthemicola*, and the ex-holotype strain *P. vinacea*.

***Paraphoma chlamydocopiosa* sp. nov.** A. Moslemi & P.W.J. Taylor, sp. nov.

MycoBank: MB819496

Etymology: Named after the abundant production of chlamydospores on CHA and PDA; *chlamydocopiosa = chlamydo* (chlamydospore) and *copiosa* (abundant) in Latin.

Morphological and cultural characteristics

On PDA

Colony diameter 17.5 mm after 1 week; aerial mycelium compact, white to greyish. Colony pigmentation after 2 weeks olivaceous grey with pale vinaceous margins. Reverse pale vinaceous to black in the centre. Margins regular.

Conidiomata pycnidial, ostiolate, unilocular and solitary, submerged in agar, mostly globose and obpyriform, brown to dark brown; 140–150 µm diam. and setose. Conidial matrix buff; pycnidial cell wall 15 µm diam., micropycnidia abundant and submerged in the medium, pale to dark brown; 70–104 µm diam. *Conidiophores* reduced to phialidic *conidiogenous cells*, hyaline, smooth and ampulliform, 6–7 µm length. *Conidia* aseptate, ellipsoid to oblong, 3–4 × 6–9 (SD = 0.31 × 2.47) µm. *Chlamydospores* abundant, occurring mostly in long chains, pale to dark brown, ellipsoid to globose and aseptate, 10–15 µm diam. (Fig. 2).

Sexual morph not observed.

On V8

Colony diameter 15 mm after 1 week; aerial mycelium woolly, silver olivaceous. Colony pigmentation after 2 weeks pale grey olivaceous with thin white margins. Reverse similar. Margins regular. *Conidia* aseptate, ellipsoid to oblong, 3–5.5 × 7–9 (SD = 0.81 × 0.61) µm.

On OA

Colony diameter 17.5 mm after 1 week; aerial mycelium floccose, green olivaceous. Colony pigmentation after 2 weeks pale olivaceous. Reverse with pale vinaceous rings formed in the centre of the colony. Margins regular.

On MEA

Colony diameter 12 mm after 1 week; aerial mycelia white-greyish and floccose. Colony pigmentation after 2 weeks dark grey to black in the centre with pale olivaceous margins. Reverse olivaceous-grey with scarlet red concentric rings in the centre. Margins regular.

On CHA

Colony diameter 12 mm after 1 week; aerial mycelium floccose, white to pale green. Colony pigmentation after 2 weeks, dark grey on both sides and pale vinaceous to black in the centre of the reverse side. Margins regular or slightly regular.

Physiological characters

No change of colour was observed upon application of 1 M NaOH to mycelium growing on OA (Dorenbosch, 1970; Boerema *et al.*, 2004). No change of colour was observed in cell wall upon application of iodine to squashed pycnidia on PDA, although the cell contents turned red, hence the cell wall type was identified as pseudoparenchymatous (*Phoma* methodologies, http://www.q-bank.eu).

Specimen examined

Holotype: Australia, northern Tasmania, Table Cape, from *Tanacetum cinerariifolium*, 2013, N. Vaghefi (BRIP 65168, culture ex-holotype - UMPc01).

Notes: Differs from *P. chrysanthemicola* described by Boerema *et al.* (2004) (*conidia* (3.5–) 4–5.5 (–6.5) × 1.5–2 (–2.5) µm) and *P. vinacea* by Moslemi *et al.* (2016) by significantly larger conidia on PDA and abundant production of chlamydospores mainly on CHA and PDA. *Paraphoma chlamydocopiosa* produces red pigmentation on PDA, OA, MEA and CHA

similar to *P. vinacea*, but with less intensity. Compact colonies of *P. chlamydocopiosa* on PDA, hardly show the vinaceous colour. *Paraphoma chrysanthemicola* produces yellow pigmentation on OA (Johnston, 1981), which does not occur in cultures of *P. chlamydocopiosa*. *Paraphoma chlamydocopiosa* colonies produced red pigmentation under UV light. This did not occur with the colonies grown in the dark.

***Paraphoma pye* sp. nov.** A. Moslemi & P.W.J. Taylor, sp. nov.

MycoBank: MB819470

Etymology: Named after the local colloquial name used to refer to pyrethrum.

Morphological and cultural characteristics

On OA

Colony diameter 22 mm after 1 week; aerial mycelium woolly, white to greyish. Colony pigmentation after 2 weeks dark olivaceous grey in the centre with white thin margins. Reverse grey-green margins turning dark olivaceous towards the centre. Margins regular.

Conidiomata pycnidial, ostiolate with long neck, 101–112 µm diam. , uni- or bilocular and solitary; submerged in agar, obpyriform, semipilose, pale to dark brown; 200–267 µm diam. Conidial matrix buff; pycnidial cell wall 10–11.5 µm thick, micropycnidia sparse, submerged in the medium, dark brown. *Conidiophores* reduced to phialidic *conidiogenous cells*, hyaline, smooth and ampulliform, 6–10 µm long. *Conidia* aseptate, ellipsoid to oblong, 3.5–6 × 1.5–3.5 (SD = 0.42 × 0.45) µm. *Chlamydospores* abundant, occurring in two types of short and long chains; and pseudosclerotioid chlamydospores (resembling pseudosclerotia forming from aggregation of unicellular chlamydospores) (http://www.q-bank.eu/); pale brown, ellipsoid to globose and aseptate, 6–8.5 µm diam. (Fig. 3).

Sexual morph not observed.

On MEA

Colony diameter 20 mm after 1 week; aerial mycelia pale grey and woolly. Colony pigmentation after 2 weeks army green in the centre with thin white margins. Reverse, similar

with dark black pigmentation towards the centre. Margins regular. *Conidia* aseptate, ellipsoid to oblong, 4–5.5 × 2–3 (SD = 0.31 × 0.38) µm.

On CHA

Colony diameter 16 mm after 1 week; aerial mycelium woolly, white to pale green. Colony pigmentation after 2 weeks, dark olivaceous on both sides turning black in centre on reverse. Margins regular. *Conidia* aseptate, ellipsoid to oblong, 3.5–5 × 1.5–3 (SD = 0.25 × 0.41) µm.

On PDA

Colony diameter 20 mm after 1 week and aerial mycelium compact, white to pale grey. Colony pigmentation dark green with white thin margins averse and black on reverse. Margins regular. *Conidia* aseptate, oblong, 3.5–6.5 × 1.5–3 (SD = 0.54 × 0.44) µm.

On V8

Colony diameter 20 mm after 1 week and aerial mycelium floccose, pale green-grey with white thin and regular margins averse and dark grey reverse. *Conidia* aseptate, oblong or ellipsoid, 3–6.5 × 1.5–3 (SD = 0.42 × 0.43) µm.

Physiological characters

No change of colour upon application of 1 M NaOH to mycelium growing on OA (Dorenbosch, 1970; Boerema *et al.*, 2004). No change of colour was observed in cell wall upon application of iodine to squashed pycnidia on PDA, although the cell contents turned red, hence the cell wall type was identified as pseudoparenchymatous (*Phoma* methodologies, http://www.q-bank.eu).

Specimen examined

Holotype: Australia, northern Tasmania, Table Cape, from *Tanacetum cinerariifolium*, 2013, N. Vaghefi (BRIP 65170, culture ex-holotype UMPp02).

Notes: Differs from *P. chrysanthemicola* described by Boerema *et al.* (2004) (*conidia* (3.5–) 4–5.5 (–6.5) × 1.5–2 (–2.5) µm) and *P. vinacea* by Moslemi *et al.* (2016) by occasional production of bilocular pycnidia on PDA and CHA. *Paraphoma pye* produces sclerotioid chlamydospores that also can be produced by the ex-neotype species, *P. chrysanthemicola*. No red pigmentation occurs in the cultures of *P. pye*. *Paraphoma chrysanthemicola* produces

yellow pigmentation on OA (Johnston, 1981), which does not occur in cultures of *P. pye*. The pycnidial cell wall is considerably thinner than that of *P. vinacea* and the ostioles have elongated necks.

Pathogenicity tests

Root inoculation

All *Paraphoma* isolates significantly reduced growth of pyrethrum plants after root dip inoculation.

All three *Paraphoma* species were able to cause upper root and crown infection, while basal petiole infection also occurred in plants inoculated with *P. pye* and *P. vinacea*. The disease incidence of *P. vinacea* was the highest compared to *P. chlamydocopiosa* and *P. pye*. *Paraphoma vinacea* infected crown and upper root tissues of all the plants in the first experiment and basal petiole, crown and root tissues of 90% of the inoculated plants in the second experiment. Upper root and crown infection with *P. chlamydocopiosa* occurred in 60% of the inoculated plants in the first experiment and 50% in the second experiment. *Paraphoma pye* infected crown and upper root tissues of 60% of the plants in the first experiment and basal petiole, crown and upper root tissues of 70% in the second experiment. No *Paraphoma* isolates were recovered from leaves, nor from any tissues of plants inoculated with water in either experiment (Table 3). Crown discoloration of plants infected with *P. chlamydocopiosa*, *P. pye* and *P. vinacea* was also observed in the root dip inoculated plants.

Paraphoma chlamydocopiosa, *P. pye* and *P. vinacea* were able to significantly reduce above ground, below ground and total biomass of the root dip inoculated plants (Table 4).

Infection by all the *Paraphoma* species significantly reduced above ground, below ground and total biomass relative to the control; however, biomass values for each species were very similar and not significantly different from each other.

Leaf and petiole inoculation

Two weeks after spray inoculation of the plants *in vivo* with *P. chlamydocopiosa* and *P. pye*, necrotic leaf lesions developed on both sides of the leaves and petioles. However, lesions

were small and did not coalesce. No leaf symptoms were observed on the plants inoculated with *P. vinacea*.

Paraphoma chlamydocopiosa caused reddish-brown and water-soaked, necrotic lesions mostly in the middle of the leaves (Fig. 4), while lesions produced by *P. pye* were yellowish to pale brown and caused margins of the leaf to curl (Fig. 5). However, results from the *in vitro* infection showed that all three species were able to cause lesions similar to those described for *in vivo* inoculation (Figs 4 & 5). No symptoms were observed on the control plants in *in vivo* or *in vitro* experiments.

Discussion

Two new pathogenic species of *Paraphoma*, *P. chlamydocopiosa* and *P. pye*, were identified from phylogenetic studies and morphological characters, and their pathogenicity as leaf and crown rot pathogens was confirmed. The three-gene PHYML phylogenetic tree of ITS-*EF1*-*TUB* separated *P. chlamydocopiosa* isolates into a well-supported monophyletic clade, and although *P. pye* clustered with *P. vinacea* there was significant bootstrap support and morphological differences to support a new species. Moreover, morphological differences were observed between *P. chlamydocopiosa* and *P. pye* isolates. *Paraphoma chlamydocopiosa* produced longer conidia than *P. pye* and *P. vinacea*. Red pigmentation of the colonies of *P. chlamydocopiosa* on OA, MEA and CHA was similar to *P. vinacea* but less intense and no red pigmentation was observed in the colonies of *P. pye* on any of the three different media. *Paraphoma pye* produced distinctive bilocular pycnidia, which did not occur in *P. chlamydocopiosa* or *P. vinacea*.

Pathogenicity of these species on pyrethrum was also confirmed *in vivo* and *in vitro* in pathogenicity trials. Above-, below-ground and total biomass were significantly reduced by *P. chlamydocopiosa*, *P. pye* and *P. vinacea* in both glasshouse root dip inoculation experiments. Pathogenicity of *Paraphoma vinacea* to pyrethrum was previously reported by Moslemi *et al.* (2016). *Paraphoma chlamydocopiosa* and *P. pye* also produced leaf lesions in glasshouse bioassays whereas *P. vinacea* did not. However, all three pathogens were able to cause leaf symptoms in inoculated detached leaves and petioles *in vitro* so may be regarded as both foliar and crown rot pathogens. It has been confirmed that *P. vinacea* is a severe crown and root rot pathogen of pyrethrum (Moslemi *et al.*, 2016). Under favourable

environmental conditions in the field, *P. chlamydocopiosa* and *P. pye* may be able to infect leaves of pyrethrum plants and cause foliar necrotic lesions, hence the reported isolation of *P. pye* or *P. chlamydocopiosa* (*P. chrysanthemicola*) in field surveys (Hay *et al*., 2015).

Aveskamp *et al.* (2008) reported that species of *Phoma* are dispersed easily by wind, water splash or birds. Therefore, it is probable that *P. chlamydocopiosa* and *P. pye* can be readily spread long distances through the fields in Tasmania under high rainfall. Therefore, each treatment was separately allocated to each group of 10 plants in the root dip inoculation experiments to avoid cross-contamination and spread of the spores via water splash in the glasshouse. Experiments were independently repeated to achieve true replication. This permitted an estimation of the variability within a treatment and the statistical inference. In addition, inoculated but noninfected plants were excluded from the analyses to reduce the measurement error.

In Hay *et al.* (2015), *P. chlamydocopiosa* was misidentified as *P. chrysanthemicola* and thus it is unlikely that *P. chrysanthemicola* exists in pyrethrum fields in Australia. This has important biosecurity implications for the introduction of *Chrysanthemum* or other hosts into Australia that may be infected with *P. chrysanthemicola*, as it has been reported on *Chrysanthemum morifolium*, but its pathogenicity is unknown on pyrethrum. Hay *et al*. (2015) reported low frequency of isolation (<7.7%) of *P. chlamydocopiosa* or *P. pye* (*P. chrysanthemicola*) from the leaf lesions in northern Tasmania in 2012. However, these pathogens were prevalent in 26% and 48% of commercial fields surveyed in spring 2012 and 2013, respectively, suggesting that either or both of these pathogen(s) are relatively widespread throughout the cropping region (Hay *et al.*, 2015). Further research needs to be carried out in order to determine the extent of infection of pyrethrum plants by *P. chlamydocopiosa* and *P. pye* in the fields.

Most previously recognised species of *Paraphoma* are soilborne and cause root and crown diseases (Boerema *et al.*, 2004; Moslemi *et al.*, 2016) except for *P. dioscoreae*, which was first isolated from the leaves of *Dioscorea tokoro* in South Korea in 2003 (Quaedvlieg *et al.*, 2013). *Paraphoma chrysanthemicola* has been shown to cause root and basal stem rot in North America and western Europe, and may cause damping-off of seedlings. It is known as the cause of stunted roots of black salsify (*Scorzonera hispanica*), and various Asteraceae in Belgium (De Gruyter *et al.*, 2010). Species of *P. radicina* have been reported as saprophytes on root surfaces of monocotyledonous plants (Gramineae, Amaryllidaceae, Iridaceae,

Liliaceae, Orchidaceae and Zingiberaceae) in Australia, Eurasia and North and South America; and in soil and on animal and inorganic substrates (De Gruyter *et al.*, 2010). *Paraphoma vinacea* was also recovered from necrotic crown and root tissues of pyrethrum in northern Tasmania (Moslemi *et al.*, 2016). *Paraphoma fimeti* has a broad host range on various plant families and has been isolated from diverse substrates.

In conclusion, *Paraphoma chlamydocopiosa* and *P. pye* were described as two new pathogens of pyrethrum, causing necrotic leaf lesions and crown rot of pyrethrum plants. However, the role of these pathogens as foliar or crown rot pathogens associated with yield decline in the fields of northern Tasmania needs to be further assessed.

Acknowledgements

The authors would like to thank Botanical Resources Australia – Agricultural Services Pty Ltd for providing pyrethrum seedlings and supplementary funding for this project. Thanks also to the University of Melbourne for Melbourne International Research Scholarship (MIRS) and Melbourne International Fee Remission Scholarship (MIFRS), which supported A.M. during this study.

References

Aveskamp MM, De Gruyster J, Crous PW, 2008. Biology and recent developments in the systematics of Phoma, a complex genus of major quarantine significance. *Fungal Diversity* **31**, 1–18.

Aveskamp MM, De Gruyter J, Woudenberg JH, Verkley GJ, Crous PW, 2010. Highlights of the *Didymellaceae*: A polyphasic approach to characterise *Phoma* and related pleosporalean genera. *Studies in Mycology* **65**, 1–60.

Barimani M, Pethybridge SJ, Vaghefi N, Hay FS, Taylor PWJ, 2013. A new anthracnose disease of pyrethrum caused by *Colletotrichum tanaceti* sp. nov. *Plant Pathology* **62**, 1248–57.

Bhuiyan MB, Groom T, Nicolas ME, Taylor PWJ, 2017. Infection process of

Stagonosporopsis tanaceti in pyrethrum seed and seedlings. *Plant Pathology* **66**. Doi: 10.1111/ppa.12622.

Boerema GH, De Gruyter J, Noordeloos ME, Hamers MEC, 2004. *Phoma Identification Manual: Differentiation of Specific and Infra-Specific Taxa in Culture*. Wallingford, UK: CABI Publishing.

Chen Q, Jiang JR, Zhang GZ, Cai L, Crous PW, 2015. Resolving the *Phoma* enigma. *Studies in Mycology* **82**, 137–217.

Crous PW, Gams W, Stalpers JA, Robert V, Stegehuis G., 2004. MycoBank: an online initiative to launch mycology into the 21st century. *Studies in Mycology* **50**, 19–22.

Crous PW, Verkley GJM, Groenewald JZ, Samson RA, 2009. *Fungal Biodiversity. CBS Laboratory Manual Series 1*. Utrecht, Netherlands: CBS-KNAW Fungal Biodiversity Centre.

De Gruyter, Woudenberg JH, Aveskamp MM, Verkley GJ, Groenewald JZ, Crous PW, 2010. Systematic reappraisal of species in *Phoma* section *Paraphoma*, *Pyrenochaeta* and *Pleurophoma*. *Mycologia* **102**, 1066–81.

De Gruyter, Woudenberg JHC, Aveskamp MM, Verkley GJM, Groenewald JZ, Crous PW, 2013. Redisposition of phoma-like anamorphs in Pleosporales re-evaluation. *Studies in Mycology* **75**, 1–36.

Dorenbosch MJ, 1970. Key to nine ubiquitous soil-borne phoma-like fungi. *Persoonia* **6**, 1–14.

Ge X, Zhou R, Yuan Y, Xu H, Fu H, Li H, 2016. Identification and characterization of *Paraphoma chrysanthemicola* causing leaf spot disease on *Atractylodes japonica* in China. *Journal of Phytopathology* **164**, 372–7.

Grdisa M, Carovic-Stanko K, Kolak I, Satovic Z, 2009. Morphological and biochemical diversity of dalmatian pyrethrum (*Tanacetum cinerariifolium* (Trevir.) Sch.Bip.). *Agriculturae Conspectus Scientificus* **74**, 73–80.

Guindon S, Gascuel O, 2003. A simple, fast, and accurate algorithm to estimate large phylogenies by maximum likelihood. *Systematic Biology* **52**, 696–704.

Hay FS, Gent DH, Pilkington S, Pearce TL, Scott JB, Pethybridge SJ, 2015. Changes in distribution and frequency of fungi associated with foliar diseases complex of pyrethrum in Australia. *Plant Disease* **9**, 1227–35.

Johnston PR, 1981. *Phoma* on New Zealand grasses and pasture legumes. *New Zealand Journal of Botany* **19**, 173–86.

Kearse M, Moir R, Wilson A *et al.*, 2012. GENEIOUS basic: an integrated and extendable desktop software platform for the organization and analysis of sequence data. *Bioinformatics* **28**, 1647–9.

Moslemi A, Ades P, Groom T, Crous PW, Nicolas ME, Taylor PWJ, 2016. Paraphoma crown rot of pyrethrum (*Tanacetum cinerariifolium*). *Plant Disease* **100**, 2363–9.

Moslemi A, Ades PK, Groom T, Nicolas ME, Taylor PWJ, 2017. *Fusarium oxysporum* and *Fusarium avenaceum* associated with yield-decline of pyrethrum in Australia. *European Journal of Plant Pathology*. Doi: 10.1007/s10658-017-1161-5.

O'Malley TB, Hay FS, Scott JB, Gent DH, Shivas RG, Pethybridge SJ, 2015. Carpogenic germination of sclerotia of *Sclerotinia minor* and ascosporic infection of pyrethrum flowers. *Canadian Journal of Plant Pathology* **37**, 179–87.

Pearce TL, Scott JB, Crous PW, Pethybridge SJ, Hay FS, 2015. Tan spot of pyrethrum is caused by a *Didymella* species complex. *Plant Pathology* **65**, 1170–84.

Pethybridge SJ, Jones SJ, Shivas RG, Hay FS, Wilson CR, Groom T, 2008. Tan spot: a new disease of pyrethrum caused by *Microsphaeropsis tanaceti* sp. nov. *Plant Pathology* **57**, 1058–65.

Quaedvlieg W, Verkley GJM, Shin HD *et al.*, 2013. Sizing up *Septoria*. *Studies in Mycology* **75**, 307–90.

Rayner RW, 1970. *A Mycological Colour Chart*. Kew, UK: Commonwealth Mycological Institute.

Srivastava SNS, 1953. On the occurrence of *Phoma chrysanthemicola* Hollos on *Chrysanthemum* sp. *Current Sciences Journal* **22**, 216.

Swofford DL, 2003. *PAUP*. Phylogenetic Analysis Using Parsimony (*and Other Methods)*. Version 4. Sunderland, MA, USA: Sinauer Associates.

Tamura K, Stecher G, Peterson D, Filipski A, Kumar S, 2013. MEGA 6: molecular evolutionary genetics analysis Version 6.0. *Molecular Biology and Evolution* **30**, 2725–7.

Vaghefi N, Hay FS, Pethybridge SJ, Ford R, Taylor PWJ, 2016. Development of a multiplex PCR diagnostic assay for the detection of *Stagonosporopsis* species associated with ray blight of Asteraceae. *European Journal of Plant Pathology* **146**, 581–95.

de Vienne DM, Giraud T, Martin OC, 2007. A congruence index for testing topological similarity between trees. *Bioinformatics* **23**, 3119–24.

Figure legends

Figure 1 Maximum likelihood PHYML combined phylogenetic tree inferred from internal transcribed spacer (ITS), translation elongation factor 1-α (*EF1-α*) and β-tubulin (*TUB*). Highest log likelihood −2871.0461. The analysis involved 31 nucleotide sequences of *Paraphoma* isolates described in this study and reference isolates obtained from GenBank. The neighbour joining bootstrap value is shown on the left only where it differs from the PHYML support value. Bootstrap values of 75% or greater are shown. Scale bar indicates expected changes per site. Host column refers to the original host where the pathogens were first isolated.

Figure 2 *Paraphoma chlamydocopiosa* (BRIP 65168) (a), (b) and (c) colony morphology and pigmentation on OA, MEA and CHA, respectively; (d) globose pycnidia on PDA; (e) pycnidial cell wall; (f) *conidiogenous* cells on PDA; (g) ellipsoid and oblong conidia on PDA; (h) micropycnidia on OA; (i) chains of chlamydospores on CHA. Scale bars (d) 200 µm, (e) 20 µm, (f) 5 µm, (g) and (i) 10 µm, (h) 100 µm.

Figure 3 *Papraphoma pye* (BRIP 65169) (a), (b) and (c) colony morphology and pigmentation on OA, MEA and CHA, respectively; (d) bilocular pycnidium on OA; (e) unilocular pycnidium on OA; (f), (g) and (h) cross sections of a pycnidium (6 µm thickness); (i) oblong and ellipsoid conidia on OA; (j) sclerotioid chlamydospores on OA; (k)

chlamydospores in chain. (l)–(m) *Conidiogenous* cells on OA. Scale bars (d,e) 200 µm, (f,g) 100 µm, (h,i) 10 µm, (j,k) 20 µm, (l,m) 5 µm.

Figure 4 Symptoms caused by *Paraphoma chlamydocopiosa* (BRIP 65168) in *in vivo* and *in vitro* experiments; (a)–(c) necrotic lesions caused by *P. chlamydocopiosa* on detached leaves and petioles *in vitro*, 8 days after inoculation; (d) a transverse section of crown tissues showing discolouration caused by *P. chlamydocopiosa*, 2 months after root dip inoculation; (e) reddish-brown necrotic leaf lesion on both sides of the leaves, 2 weeks after spray inoculation of the leaves *in vivo.*

Figure 5 Symptoms caused by *Paraphoma pye* (BRIP 65169) in *in vivo* and *in vitro* experiments. (a)–(b) Dark brown to black necrotic lesions caused by *P. pye* on detached leaves and petioles *in vitro*, 8 days after inoculation; (c) marginal chlorosis of the leaves, 2 weeks after spray inoculation *in vivo*; (d) necrosis of the newly grown petioles *in vivo*, 2 weeks after spray inoculation.

Table 1 Information of the location in Tasmania (Australia), field code, collectors and dates in which new Paraphoma isolates from pyrethrum (Tanacetum cinerariifolium) used in this study were recovered

Acc. number	Species	Date isolated	Collector	Field code	Region
BRIP 57988	P. chlamydocopiosa	2012-08-06	T. Pearce	70042	Table Cape
BRIP 65178	P. chlamydocopiosa	2012-08-14	T. Pearce	70042	Table Cape
BRIP 57989	P. chlamydocopiosa	2012-08-21	T. Pearce	51907	East Devonport
BRIP 65177	P. chlamydocopiosa	2012-08-27	T. Pearce	70046	Table Cape
BRIP 65173	P. chlamydocopiosa	2012-08-27	T. Pearce	57348	Wesley Vale
BRIP 65176	P. chlamydocopiosa	2013-07	F. Hay	48303	North Motton
BRIP 65179	P. chlamydocopiosa	2014-07-21	J. Scott	82205	Circular Head
BRIP 65174	P. chlamydocopiosa	2014-09-23	J. Scott	87402	Wynyard
BRIP 65168	P. chlamydocopiosa	2013	N. Vaghefi	70047	Table Cape
BRIP 65170	P. chlamydocopiosa	2013	N. Vaghefi	70047	Table Cape
BRIP 65169	P. pye	2013	N. Vaghefi	70047	Table Cape
BRIP 65171	P. pye	2013	N. Vaghefi	70047	Table Cape
BRIP 63682	P. vinacea	2014-06	A. Moslemi	64209, 49206	Devonport
BRIP 63683	P. vinacea	2014-07	A. Moslemi	49207, 74201	Devonport
BRIP 63684	P. vinacea	2014-08	A. Moslemi	47110, 46410	Devonport
BRIP 63685	P. vinacea	2014-09	A. Moslemi	86901	Devonport

Table 2 Collection details and GenBank accession numbers of isolates

Isolate	Strain/culture collection no.[c]	Substrate	Location	GenBank accession number		
				ITS	TUB	EF1
Paraphoma chrysanthemicola[a]	CBS 522.66[d]	Chrysanthemum morifolium	UK	KF251166	KF252661	KF253124
P. chrysanthemicola[a]	CBS 172.70	C. morifolium	Netherlands	KF251165	KF252660	KF253123
Paraphoma chlamydocopiosa	UMPc01; BRIP 65168	Tanacetum cinerariifolium	Australia	KU999072	KU999084	KU999080
P. chlamydocopiosa	UMPc03; BRIP 65170	T. cinerariifolium	Australia	KU999074	KU999086	KU999082
P. chlamydocopiosa	UTAS01; BRIP 57988	T. cinerariifolium	Australia	KX376282	KX376290	KX376298
P. chlamydocopiosa	UTAS02; BRIP 65174	T. cinerariifolium	Australia	KX376283	KX376291	KX376299
P. chlamydocopiosa	UTAS04; BRIP 65173	T. cinerariifolium	Australia	KX376284	KX376292	KX376300
P. chlamydocopiosa	UTAS05; BRIP 57989	T. cinerariifolium	Australia	KX376285	KX376293	KX376301
P. chlamydocopiosa	UTAS06; BRIP 65176	T. cinerariifolium	Australia	KX376286	KX376294	KX376302
P. chlamydocopiosa	UTAS07; BRIP 65177	T. cinerariifolium	Australia	KX376287	KX376295	KX376303
P. chlamydocopiosa	UTAS09; BRIP 65178	T. cinerariifolium	Australia	KX376288	KX376296	KX376304
P. chlamydocopiosa	UTAS010; BRIP 65179	T. cinerariifolium	Australia	KX376289	KX376297	KX376305
Paraphoma dioscoreae[a]	CBS 135100[d]	Dioscorea tokoro	South Korea	KF251167	KF252662	KF253125

P. dioscoreae[a]	CPC 11355	D. tokoro	South Korea	KF251168	KF252663	KF253126
P. dioscoreae[a]	CPC 11361	D. tokoro	South Korea	KF251169	KF252664	KF253127
Paraphoma fimeti[a]	CBS 170.70[d]	Apium graveolens	Netherlands	KF251170	KF252665	KF253128
P. fimeti[a]	CBS 368.91	Juniperus communis	Switzerland	KF251171	KF252666	KF253129
P. fimeti	CBS 164.31	Zea mays	Unknown	KY559063	KY559077	KY559070
P. fimeti	CBS 258.68	Wheat field soil	Germany	KY559064	KY559078	KY559071
P. fimeti	CBS 119457	Butter turned sour	Netherlands	KY559068	KY559082	KY559075
P. fimeti	CBS 550.70	Wood	Germany	KY559066	KY559080	KY559073
P. fimeti	CBS 379.67	Oil paint	France	KY559065	KY559079	KY559072
Paraphoma pye	UMPp02; BRIP 65169	T. cinerariifolium	Australia	KU999073	KU999085	KU999081
P. pye	UMPp04; BRIP 65171	T. cinerariifolium	Australia	KU999075	KU999087	KU999083
Paraphoma radicina[a]	CBS 102875[d]	Lycopersicon esculentum	Germany	KF251671	KF251671	KF251671
P. radicina[a]	CBS 111.79	Malus sylvestris	Netherlands	KF251172	KF252667	KF253130

Paraphoma vinacea[b]	UMPv001; BRIP 63684; CBS 141995[d]	T. cinerariifolium	Australia	KU176884	KU176892	KU176896
P. vinacea[b]	UMPv002; BRIP 63683	T. cinerariifolium	Australia	KU176885	KU176893	KU176897
P. vinacea[b]	UMPv003; BRIP 63682	T. cinerariifolium	Australia	KU176886	KU176894	KU176898
P. vinacea[b]	UMPv004; BRIP 63685	T. cinerariifolium	Australia	KU176887	KU176895	KU176899
Neosetophoma samarorum[a]	CBS 138.96	Phlox paniculata	Netherlands	KF251160	KF252655	KF253119

[a]Quaedvlieg et al. (2013).

[b]Moslemi et al. (2016).

[c]BRIP, Queensland Plant Pathology herbarium, Brisbane, Australia; CBS, Westerdijk Fungal Biodiversity Institute, Netherlands; CPC, Culture collection of Pedro Crous, housed at the Westerdijk Institute, Netherlands; UMPc, University of Melbourne, Paraphoma chlamydocopiosa strain; UMPp, University of Melbourne, Paraphoma pye strain; UTAS, University of Tasmania.

[d]CBS 522.66 is the ex-neotype of P. chrysanthemicola Hollos; CBS 135100 is the ex-holotype of P. dioscoreae; CBS 170.70 is the ex-neotype of P. fimeti Branaud; CBS 102875 is the ex-epitype of P. radicina (McAlpine) Morgan-Jones and J. F. White; CBS 141995 is the ex-holotype of P. vinacea Moslemi and Taylor.

Table 3 Disease incidence and tissues of pyrethrum plants infected 2 months after inoculation with *Paraphoma* chlamydocopiosa, P. pye and P. vinacea

Experiment	Inoculum	No. of replicate plants	No. of infected plants[a]	Incidence (%)			
				Leaf	Basal petiole	Crown	Root
1	Control	10	0	0	0	0	0
	P. chlamydocopiosa	10	6	0	0	10	50
	P. pye	10	6	0	0	10	50
	P. vinacea	10	10	0	0	50	80
2	Control	10	0	0	0	0	0
	P. chlamydocopiosa	10	5	0	0	30	20
	P. pye	10	7	0	40	40	0
	P. vinacea	10	9	0	40	60	40

[a]Total number of plants from which the target pathogen was recovered.

Table 4 Dry weights of the above and below ground portions of pyrethrum plants 2 months after inoculation with Paraphoma chlamydocopiosa, P. pye and P. vinacea

	Dry weight component (g)		
Treatment	Above ground	Below ground	Total
Control	7.10 a	4.52 a	11.50 a
P. chlamydocopiosa	5.31 b	2.85 b	8.29 b
P. pye	5.21 b	3.11 b	8.39 b
P. vinacea	5.73 b	3.18 b	8.91 b
$F_{3,58}$	3.73	12.82	7.54
P-value	<0.01	<0.001	<0.0002

Means with different letters in the same column are significantly different by pairwise t-tests ($\alpha = 0.05$). In all cases the F ratio for testing the treatment effect has 3 and 58 df. This was obtained by combining the two experiments and fitting a linear mixed model with different error terms in each experiment.

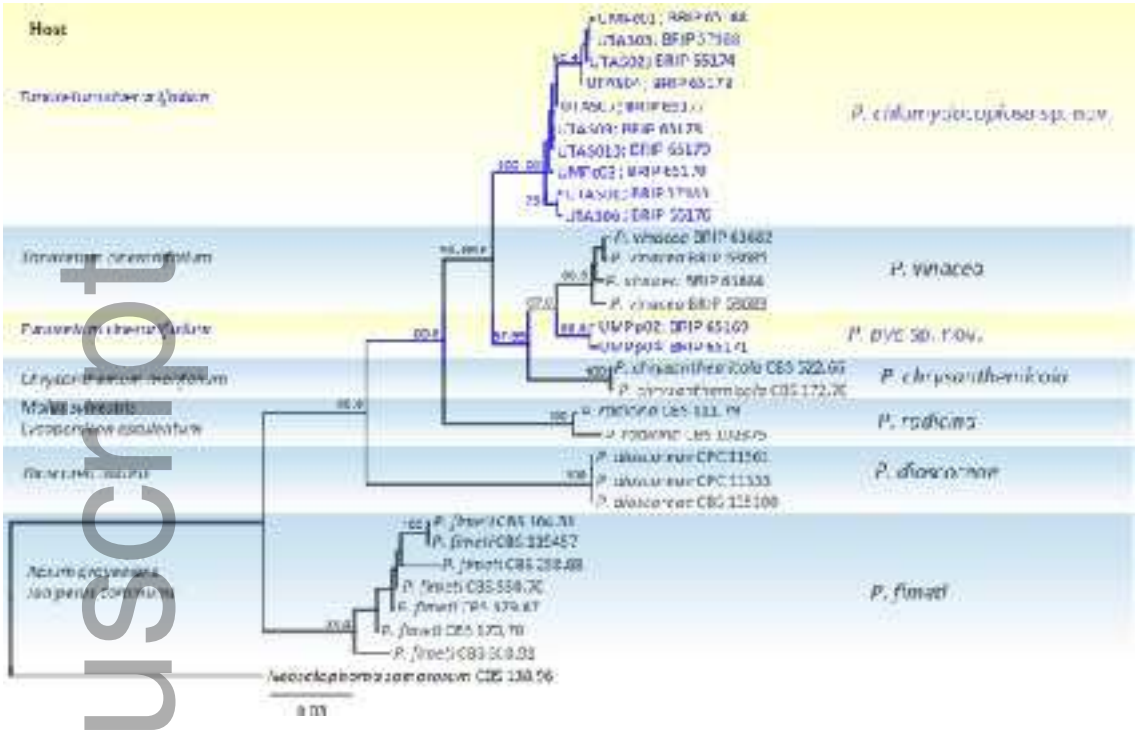

ppa_12719_f1_aa.tif

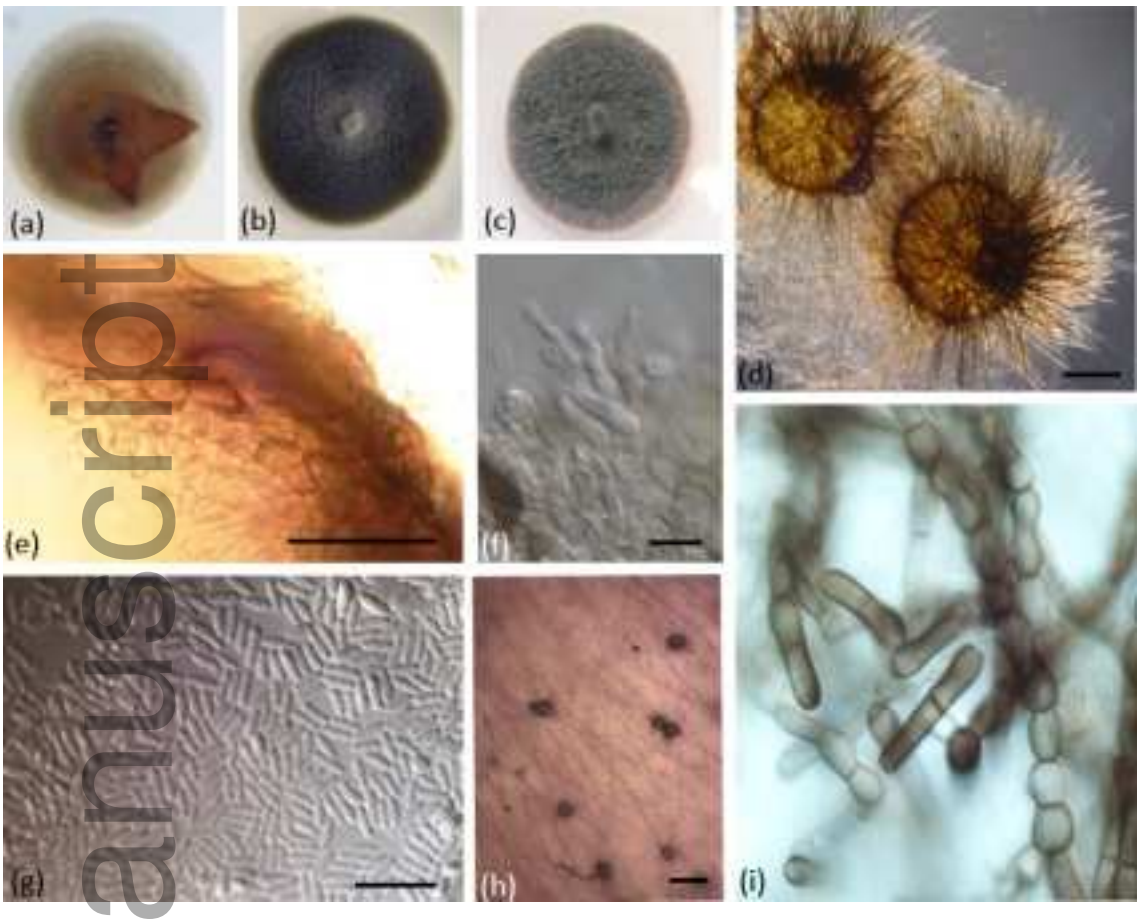

ppa_12719_f2_aa.tif

ppa_12719_f3_aa.tif

ppa_12719_f4_aa.tif

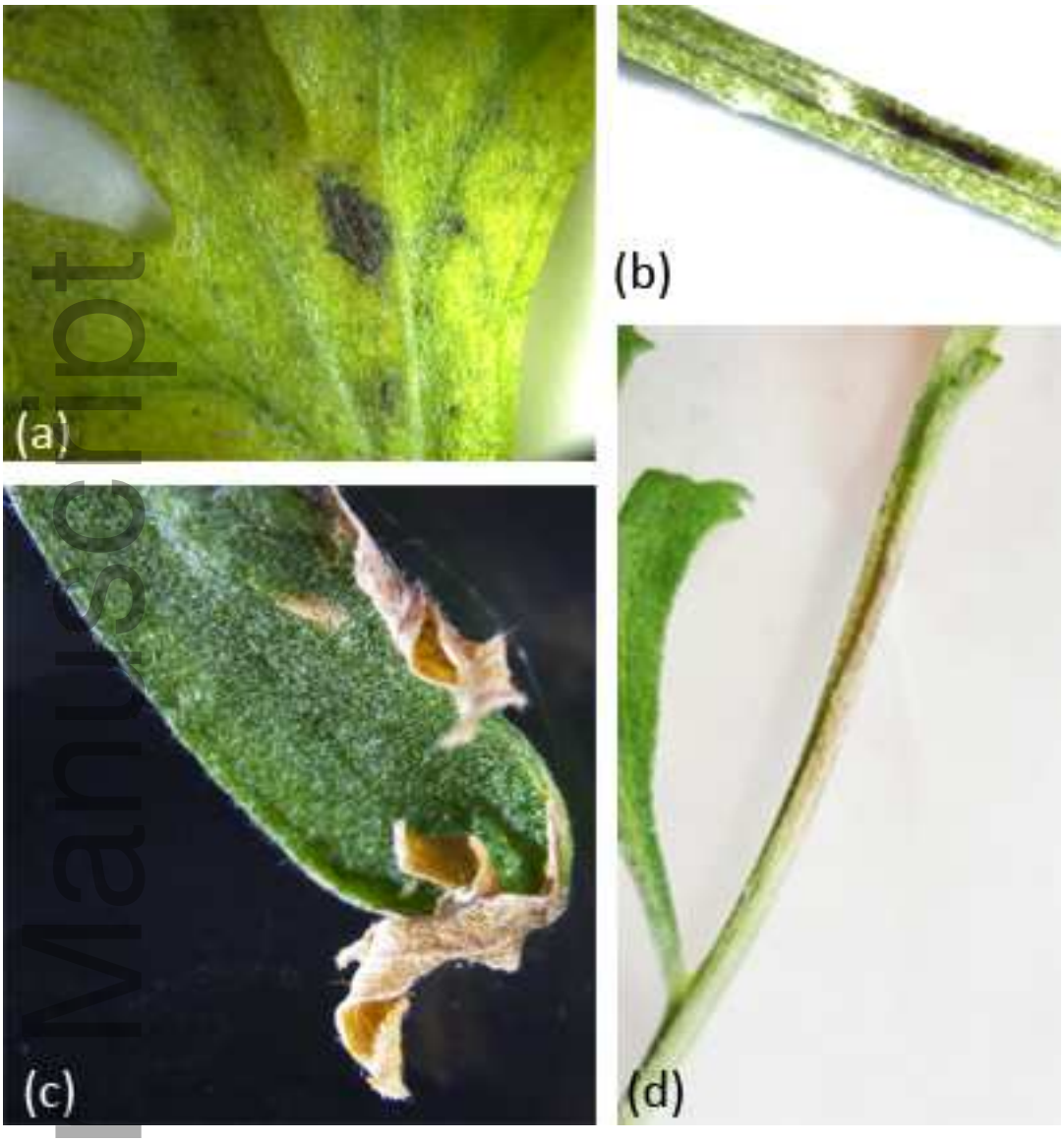

ppa_12719_f5_aa.tif

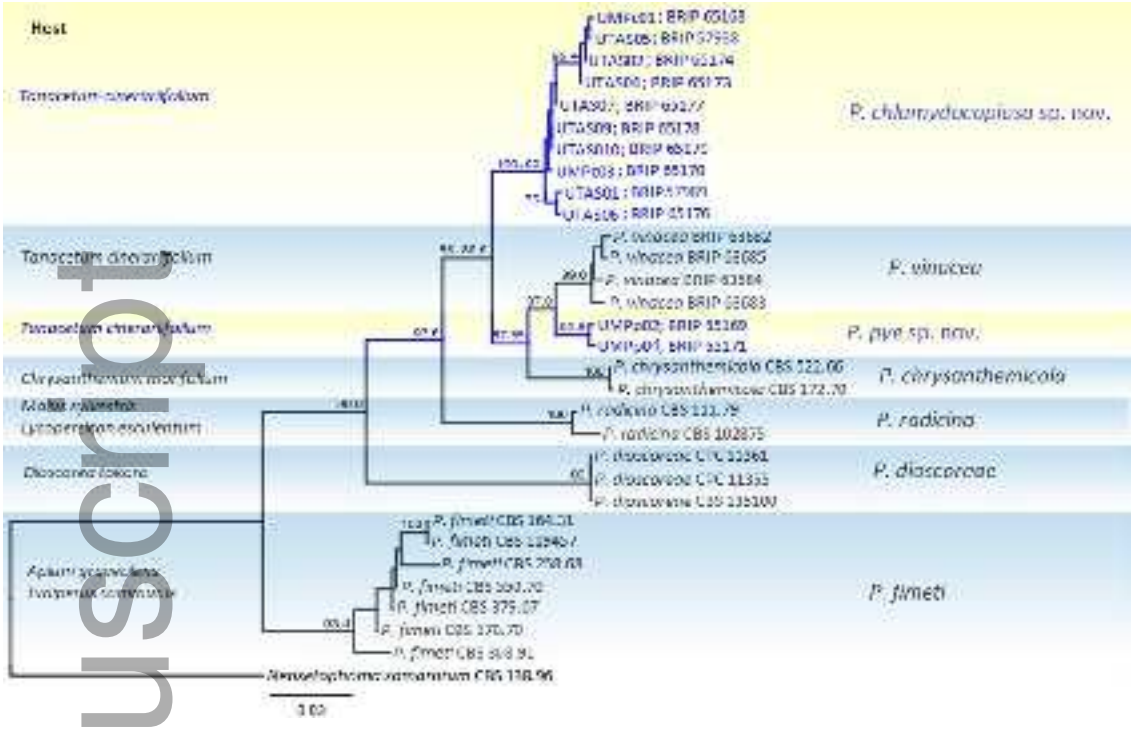

ppa_12719_f1.tif

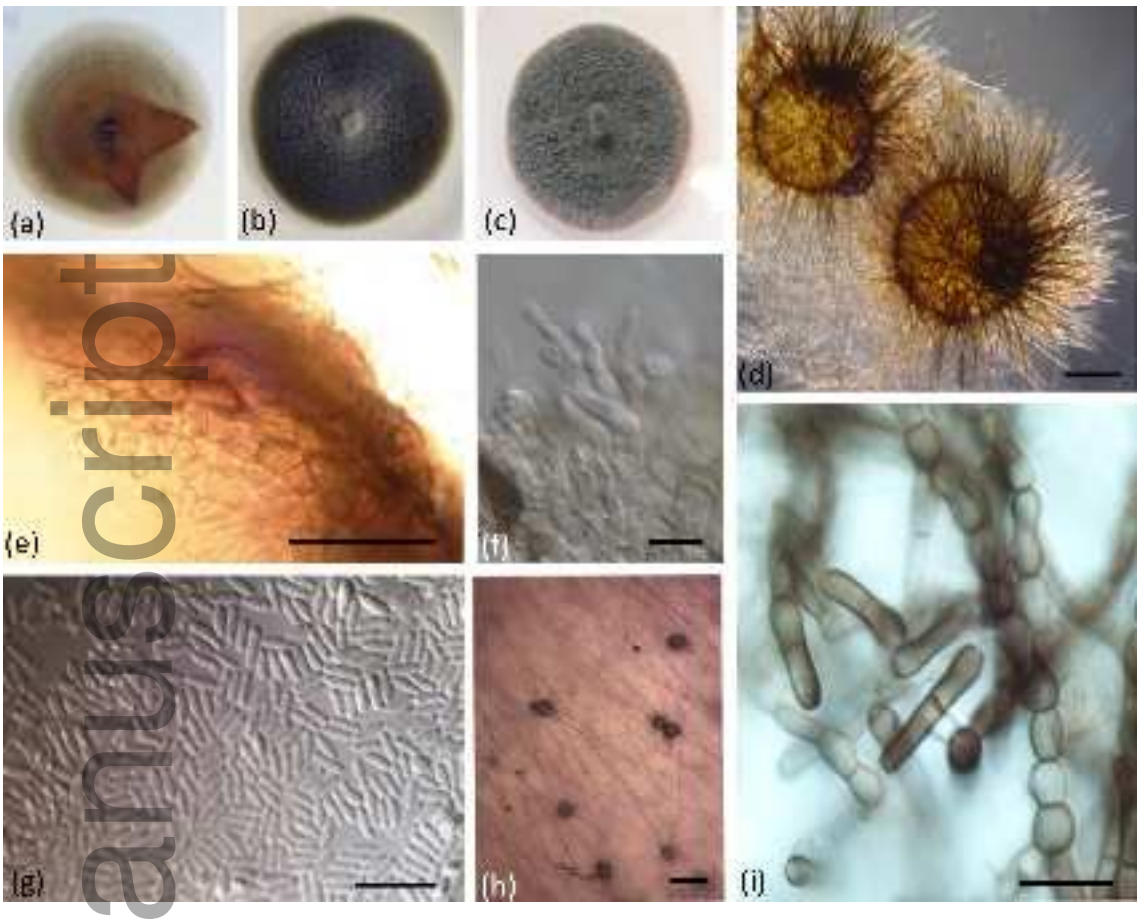

ppa_12719_f2.tif

ppa_12719_f3.tif

ppa_12719_f4.tif

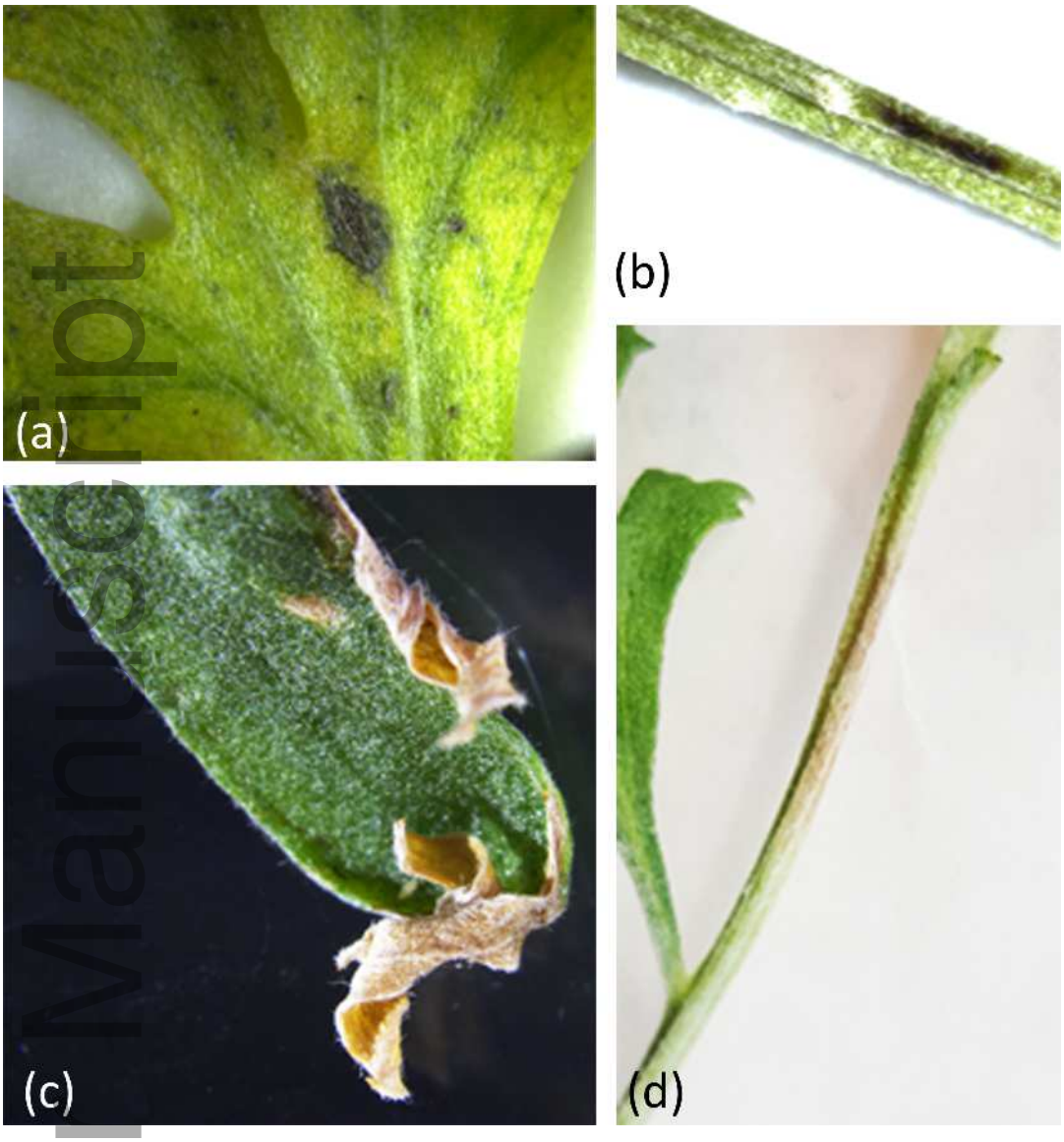

ppa_12719_f5.tif

Author/s:
Moslemi, A; Ades, PK; Crous, PW; Groom, T; Scott, JB; Nicolas, ME; Taylor, PWJ

Title:
Paraphoma chlamydocopiosa sp nov and Paraphoma pye sp nov., two new species associated with leaf and crown infection of pyrethrum

Date:
2018-01-01

Citation:
Moslemi, A., Ades, P. K., Crous, P. W., Groom, T., Scott, J. B., Nicolas, M. E. & Taylor, P. W. J. (2018). Paraphoma chlamydocopiosa sp nov and Paraphoma pye sp nov., two new species associated with leaf and crown infection of pyrethrum. PLANT PATHOLOGY, 67 (1), pp.124-135. https://doi.org/10.1111/ppa.12719.

Persistent Link:
http://hdl.handle.net/11343/292962